

PAPER V

**The chromatographic separation
of anionic dye in inkjet coating
structures**

In: *Colloids and Surfaces A: Physicochemical and
Engineering Aspects* 2011(377)1–3, pp. 304–311.
Copyright 2011 with permission from Elsevier.



The chromatographic separation of anionic dye in inkjet coating structures

T.T. Lamminmäki^{a,*}, J.P. Kettle^a, P.J.T. Puukko^a, P.A.C. Gane^{b,c}

^a VTT Technical Research Centre of Finland, P.O. Box 1000, 02044 VTT, Finland

^b Aalto University, School of Science and Technology, Faculty of Chemistry and Materials Sciences, Department of Forest Products Technology, P.O. Box 16300, FIN-00076 Aalto, Finland

^c Omya Development AG, CH-4665 Oftringen, Switzerland

ARTICLE INFO

Article history:

Received 16 November 2010

Received in revised form

21 December 2010

Accepted 7 January 2011

Available online 18 January 2011

Keywords:

Absorption

Diffusion

Porosity

Ink penetration

Thin layer chromatography

Ink dye adsorption

Inkjet printing

Coating

Mercury intrusion porosity

ABSTRACT

During the ink setting process on coated inkjet paper, the porosity and pore size distribution of the coating structure determines how much, in which direction and at what speed the surface can absorb the ink. The capillary and permeation flow drives the liquid into the structure and controls the volume flow, respectively. The coating binder, quite often polyvinyl alcohol, has an effect on the inkjet ink imbibition by occupying a proportion of the available pore volume and absorbing via swelling of the polymer matrix. The aim of this work is to clarify the role of the porous structure and the coexistent swelling of binder during the liquid imbibition, with special attention paid to the fixation of dye and its distribution during the chromatographic separation process. The results confirm that water molecules diffuse into and within hydrophilic polyvinyl alcohol binder causing the binder swelling. The swelling affects the number of active small pores remaining available for capillarity, by reducing the diameter and volume of the remaining free pores, thus slowing the capillary flow, such that the permeation flow rapidly becomes the rate determining step rather than the desired fine capillary-driven liquid imbibition. On the other hand, water molecules diffusing into the binder structure open the polymer network so that the colorant molecules can also fit into it. This mechanism is reflected in the observation that, in the case of dye-based inks, there is always a clear (non-coloured) wetting front advancing before the colour front. The swelling binder, therefore, though reducing absorption dynamic, does act to provide sorption volume and surface for colorant, aiding an otherwise coating surface area limited function in respect to dye capture and fixation.

© 2011 Elsevier B.V. All rights reserved.

1. Introduction

The penetration of inkjet ink and soluble dye colorant fixing into the structure of coated paper during imbibition is complex and cannot adequately be described by a single phenomenon, such as capillarity or direct surface adsorption alone. Fig. 1 shows one demonstration of the interaction phenomena during the inkjet ink setting process [1]. Initially, the ink droplet arrives onto the paper surface and the wetting of the paper begins. At this stage, the inertia of the droplet affects the ink movement [2,3]. The capillary force in the z-direction of paper competes with the spreading in the x,y-direction [4]. The capillary force becomes a dominating phenomenon and it forces the ink vehicle and mobile components into the pore structure. Microcapillary penetration starts typically after about 0.1 ms from the droplet arriving [5]. Nanopores in the structure (<0.1 μm), on the other hand, generate absorption with

a timescale of single pore filling of approximately 10 ns [5]. After a few milliseconds, the separation of the ink components starts and the capillary penetration continues strongly [6,7]. After about one second from the droplet arriving, the significance of liquid adsorption onto the coating structure surface increases [8]. The diffusional movement takes place already at the capillary imbibition between liquid and surface interface, but it is traditionally assumed to be a quite small effect at this stage [8]. The significance of diffusion of ink components was assumed to increase only over time as the ink has penetrated deeper into the structure [7,9]. The role of diffusion at the beginning of the inkjet ink imbibition process has not been studied in detail until very recently. Lamminmäki et al. [10], have shown that the presence of soluble and swelling binder, such as polyvinyl alcohol, reacts under water diffusion rapidly over the very short distances associated with the nanopore structure of discretely bimodally distributed pores in modern precipitated and modified calcium carbonate-based inkjet coatings [11]. At the final stages of ink setting, although inkjet inks touch dry rapidly, polymerization of pigment adhesives, if present, is nonetheless a relatively slow process, which can take the order of several hundreds of seconds, and a final drying time of the ink is in the order of hours [2].

* Corresponding author.

E-mail addresses: taina.lamminmaki@vtt.fi (T.T. Lamminmäki), john.kettle@vtt.fi (J.P. Kettle), pasi.puukko@vtt.fi (P.J.T. Puukko), patrick.gane@aalto.fi (P.A.C. Gane).

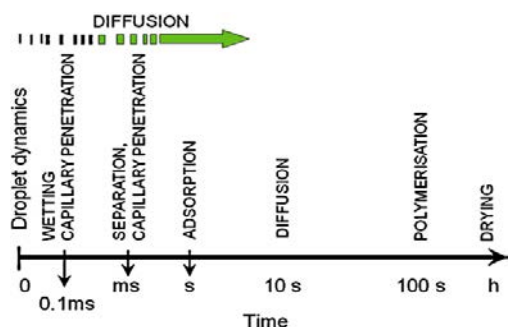


Fig. 1. The presumed interaction phenomena of the inkjet ink setting process and their relevant onset timescales [1]. Superposed, above the time spectrum, is the relatively new observation that absorbent binder, distributed within high surface nanopores, as part of discretely bimodal pore structures, acts to absorb at the short timescale also by diffusion.

Thin layer chromatography (TLC) has been utilized before in a study of inkjet ink fixing by Donigian et al. [12,13] and Glittenberg et al. [14]. In all these researches, TLC was used in the study of dye colorant fixing to the coating layer in a conventional way. A droplet of dye-based ink was spotted onto the precipitated calcium carbonate and silica coatings and allowed to dry there. In the TLC development process, the ink vehicle was used then as the eluent. The colorant and eluent front location after the development process was detected and from them was calculated the R_f value (the ratio of the distance that the substance travels to the distance that the solvent travels up the plate). They varied the content of polyvinyl alcohol and cationic additive in their study. However, the coatings did not at that time display the marked discretely bimodal pore distribution, characteristic of the fastest carbonate absorbing structures today.

The objective of this work is to establish the relationship between colorant dye charge and concentration of dye upon penetration into an inkjet coating of the colorant and vehicle, respectively. With thin layer chromatography, model calcium carbonate coatings, displaying the discretely bimodal pore structure property, are studied to illustrate a comparison of a diffusive and non-diffusive coating structure. Polyvinyl alcohol (PVOH) is used as a “diffusion driving” binder and compared with a styrene acrylate latex as a “less-diffusing”, or virtually non-diffusing, binder, where both categories of diffusion behaviour refer to the case of exposure to water.

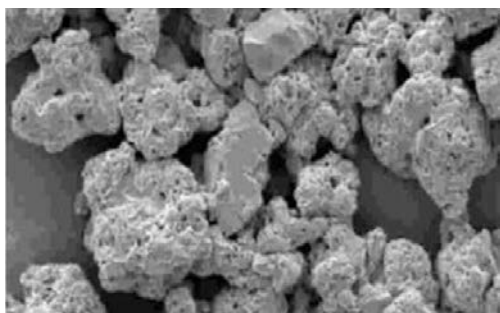


Fig. 2. The SEM picture of MCC pigment.

2. Materials and methods

2.1. Raw materials

The chosen pigment was a modified calcium carbonate (MCC), Omyjet B6606.¹ The weight median diameter of the MCC pigment particles ($d_{50\%}$) was 2.7 μm and the specific surface area, 46.2 $\text{m}^2 \text{g}^{-1}$ (BET, ISO 9277). The pigment particle provides capillary absorption capacity and high surface adsorption area via its intra-particle pores (Fig. 2). The packing of such internally porous particles develops the characteristic bimodal pore size distribution when used in the inkjet coating layer, Fig. 5. The pigment was provided by the manufacturer as a dry powder, which had some cationic dispersing agent on the surface of the pigment particles designed to be applied for coatings accepting anionic dye-based inkjet inks. Two contrasting binders were used: a non-ionic polyvinyl alcohol (PVOH, Mowiol 40-88²) and an anionically stabilized styrene acrylate latex (SA, Latexia 212³). The PVOH had a degree of hydrolysis of $87.7 \pm 1.0\%$. The latex had a particle size of 180 nm and glass transition temperature of -20°C . An anionic sodium polyacrylate (Polysalz S3, molecular weight 4000 g mol^{-1}) and a cationic poly(diallyl dimethyl ammonium chloride) (polyDADMAC, Cartafix VXU⁴) were used as dispersing and charge modifying agents, respectively.

The respective charge modifying agent (anionic dispersant and/or polyDADMAC) amount was 0.5 pph. In the case of making down anionic coating colours, the anionic dispersing agent was added into the initial water, as normal, before the cationic pigment addition, in order to “flip” the charge from cationic to anionic. The mixing of pigment and anionic dispersing agent took 30 min. Into those coating colours that were to contain binder, the PVOH or SA latex was applied next and the mixing lasted again 30 min. The coating layers had only 1 pph of binder because the chromatographic eluent movement was desired to be as free flowing as possible. In the complementary case of making down cationic colours, the addition of polyDADMAC was made after PVOH binder addition. Due to the anionic nature of the SA latex, no corresponding cationic colour using this binder was prepared.

2.2. Testing methods

In our study, the target was to detect how the dye-based colorant in water moves during the ink imbibition. Therefore, we used the thin layer chromatography (TLC) technique differently than Donigian et al. [12,13]. Coated glass plates were used as the basis for the coatings in TLC. Deionized water was the eluent in the TLC analysis and the adsorbate (substance adsorbed) was provided by a range of concentrations of anionic cyan colorant (Basacid Blue 7623, Cu phthalocyanine). The model coatings were applied to the glass plate surface using an Erichsen⁵ film applicator (Model 288). The applied coat weight was about 100 g m^{-2} . The coating layers were dried at room temperature over night. During the TLC development in our case, the term “eluent” now refers to the water phase (ink vehicle equivalent) of a solution of dye applied as a supersource reservoir, i.e. not the classical eluent travelling past a previously dried colorant, but a carrier. The distance of the eluent (water phase) movement over time was measured. Simultaneously, the gray level of surface reflectance was detected with a digital camera

¹ Omya AG, Postfach 32, CH-4665 Oftringen, Switzerland.

² Kuraray Specialities Europe GmbH, Building D 581 D-65926, Frankfurt am Main, Germany.

³ BASF Aktiengesellschaft, Paper Chemicals, 67056 Ludwigshafen, Germany.

⁴ Clariant International AG, Rothausstrasse 61, CH-4132 Muttenz 1, Switzerland.

⁵ Erichsen GmbH & Co., Am Iserbach 14, D-58675 Hemer, Germany.

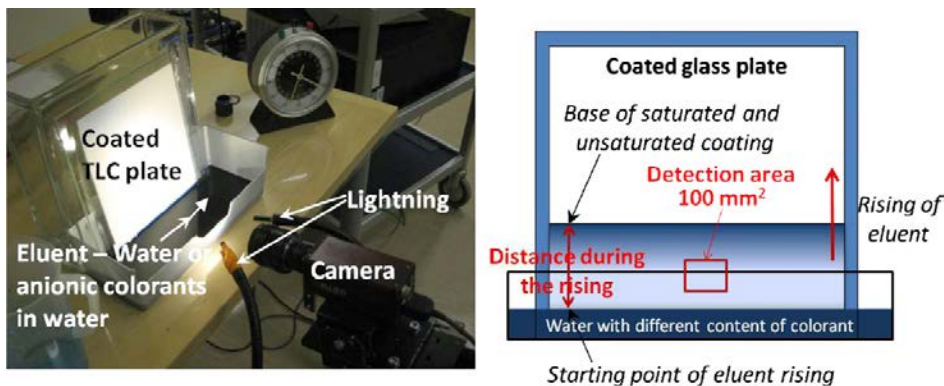


Fig. 3. The TLC development system and the location of gray value measurement and the distance of eluent front.

(Dolphin F145C⁶). The illumination of the surface was made on the same side as that viewed by the camera (Fig. 3). The measurements were made at a temperature of 20.0 ± 1.5 °C. The image analysis software Image-Pro 6.2⁷ was used and the detection area started about 0.5 mm above the advancing eluent front and the total detection area was 100 mm². The gray level of the undeveloped plate was adjusted to a gray level of 150. The distance was expressed toward the base of the TLC plate passing from unsaturated to saturated sample.

The porosities of the coating layers were analyzed by a silicon oil (Si-oil) absorption saturation method and mercury porosimetry. In the Si-oil measurement, the pigment cake was left for one hour in the oil, and the weight of cake before and after oil saturation was measured. The absorbed liquid volume was measured as the weight change between the “dry” and the saturated sample divided by the density of the silicon oil (0.934 g cm^{-3}). The density of each pigment system was also measured and this can be one reason for variation in the results. The porosity was thus defined as the volume of absorbed liquid at saturation divided by total volume of sample, all determined at room temperature and atmospheric pressure. In the mercury porosimetry (Micromeritics AutoPore IV⁸) measurement, the coating layer was impregnated with mercury using both low and high pressure. The pore volume and pore size distribution were analyzed adopting the Pore-Comp⁹ correction, which takes account for penetrometer expansion, mercury compression and compression of the sample skeletal material, expressed as the elastic bulk modulus, according to Gane et al. [15].

3. Results

3.1. Coating layer properties

Fig. 4 shows the porosity results of coating layers measured with the silicon oil absorption and mercury porosimetry. The relative accessibility for oil under imbibition and mercury under external pressure to penetrate into the coating structure resulted in some divergence in the results for porosities. It is possible that some of the coating structure was not saturated with liquid oil, especially

due to it being a non-pressurized measurement, as the presence of binder may have limited pore connectivity. The highest Si-oil porosity result was for the cationically dispersed pigment. Otherwise the results were on the same level. The porosity results of mercury porosimetry were altogether on a higher level than the results of Si-oil measurement, but they also indicated very similar porosity to those of studied coatings.

Fig. 5A shows the cumulative pore volume and Fig. 5B the pore size distribution of the coatings determined by mercury porosimetry. The first derivative of the cumulative mercury intrusion curves, although limited to a model of an equivalent bundle of capillaries, and thus ignoring pore shielding effects, is nonetheless useful for comparison purposes between topologically similar structures [16]. The MCC pigment coatings had both intra and inter-particle pores and thus results in curves of pore size distribution having two peaks (Fig. 5B). The addition of 1 pph of binder had a very minimal influence on intra-particle pores (below 70 nm). In the inter-particle pore area (over 0.1 μm), the anionic pigment with PVOH had more 0.27 μm diameter pores than the others. The largest pores were produced by the anionic coating with 1 pph SA latex (0.65 μm).

3.2. Anionic colorant movement in the swelling and non-swelling binder-containing coating

The results show that there always exists a wetting front rising within the coating structure in advance of the colorant front, and this was seen to be true for both the combinations of charge, i.e. anionic dye–cationic coating, and anionic dye–anionic coating.

At first sight, the formation of a colorant-free wetting front was unexpected for the combination of anionic colorant and anionic coating layer, as there is no obvious retardation adsorption mechanism on the basis of charge alone. The wetting water front height in this anionic case was about one millimetre ahead of the colorant front. It was also noted that the retarded colorant fronts were darker than the following (trailing) colours (Fig. 6, anionic coatings). It is concluded that as the finest pores of the coating structure drive the wetting front forward, they can be assumed to exclude the dye. This provides an important corollary, in that the surface area associated with the finest pores in these structures is either not available for adsorption of the dye, or a further rate determining step is involved. Experience suggests that the *anionic repulsion* is the primary exclusion mechanism.

In the cationic coating, the anionic colorant initially stayed at the bottom edge of the cationic coating layer in contact with the liquid reservoir. After ten minutes the fixed bottom edge appeared to fill with colorant and part of the colorant volume then started to

⁶ Allied Vision Technologies, Taschenweg 2A, D-07646, Stadtraa, Germany.

⁷ Media Cybernetics, Inc., 4340 East-West Hwy, Suite 400, Bethesda, MD 20814-4411, USA.

⁸ Micromeritics Instrument Corporation, 4536 Communications Drive, Norcross, GA 30093, USA.

⁹ Pore-Comp are a software network model and sample compression correction software, respectively, developed by the Environmental and Fluid Modelling Group, University of Plymouth, PL4 8AA, UK.

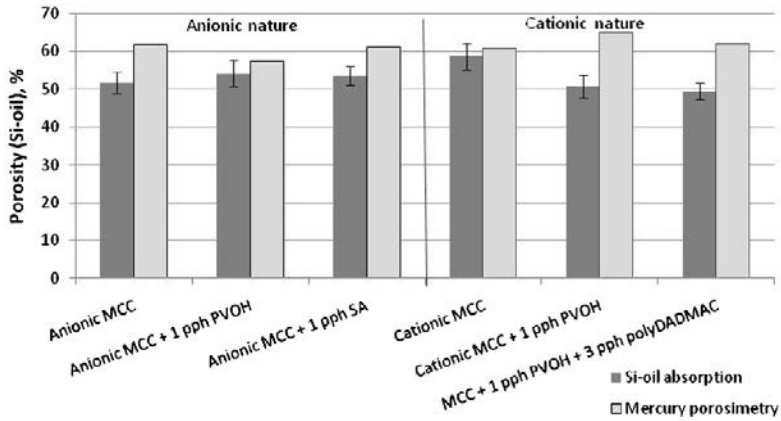


Fig. 4. Porosity of coatings measured with silicon oil absorption and mercury porosimetry.

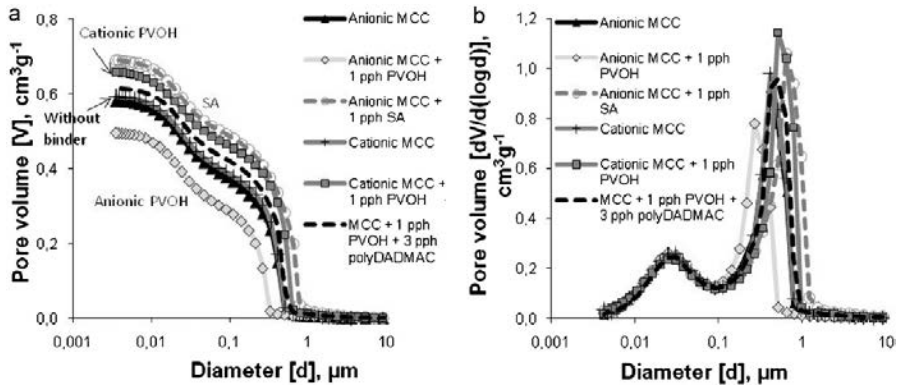


Fig. 5. The cumulative pore volume (A) and pore size distribution (B) of coatings. Measured with mercury porosimetry – an example of the discretely bimodal pore size distribution of MCC in a coating structure, generated by the nanopores within the particles and the micropores between them.

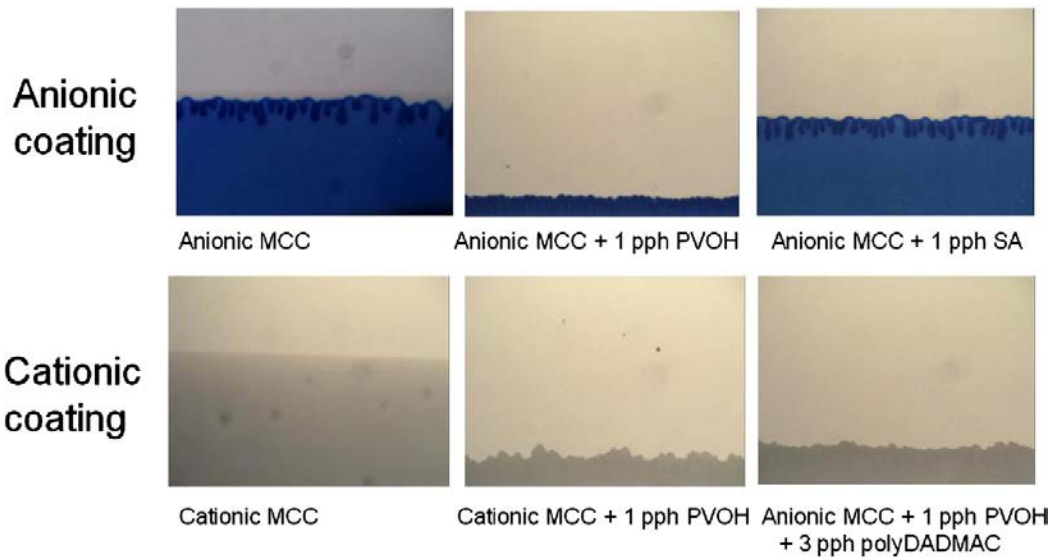


Fig. 6. The 5.0 wt% anionic cyan colorant rising within different coating layers. Measured after 4 min time delay.

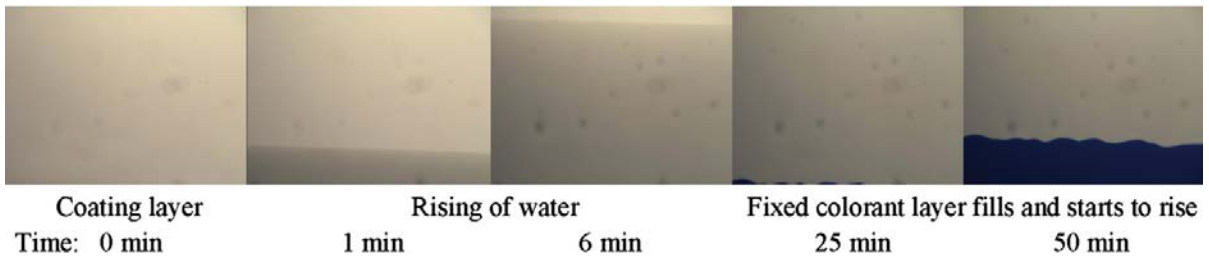


Fig. 7. Anionic colorant (5 wt%) movement on the cationic MCC TLC plate.

rise little by little: especially, this could be seen when there was a higher concentration of 5.0 wt% colorant in water (Fig. 7). Clearly, the surface area associated with the cationised pores took part in adsorption, and only when the surface area was saturated could the colorant move forward into the structure.

Fig. 8 shows the water front distance as the eluent rose through the coating structure. The highest water rising was observed in the binder-free systems. The coating with SA latex had a plateau height value roughly half that of the binder-free coating, and the lowest values were for PVOH containing coatings.

Fig. 9 shows the gray level values of MCC coatings. The eluent was pure water or water with different amounts of anionic cyan colorant. In the anionic coatings, the gray level value change was caused by the movement of water and colorant, whereas in the cationic surfaces it was caused by water movement only until adsorption saturation at a given height was reached. The change of gray value measured above the coloured region was caused by the coating layer progressively filling with water advancing ahead of the colorant: when the value is high, it means that the change toward a darker appearance on the plate was small, and when the value is low it indicates a greater darkening effect was observed. The water, and water with different colorant contents, penetrated very similar distances, as Fig. 8 indicated, in the respective coating structures, regardless of cyan colorant amount in water.

4. Discussion

The TLC development lasted quite long time, even as long as 40 min, and the evaporation of water might have some effect on the liquid movement during this time. Therefore, we detected the evaporation of water by measuring the weight change over time at

the same temperature as the TLC measurement proceeded. From this weight we calculated the effect of evaporation on the eluent distance through the TLC coating by taking account of the water density and the coating layer dimensions on the glass plate. Fig. 10 shows the evaporation rate of water, from which could be calculated the effect of evaporation on the rate of liquid. The evaporation causes at the maximum about $0.005 \text{ mm min}^{-1}$ retardation on the TLC plate, whereas in the coating layer the water moves at 3.0 mm min^{-1} at its fastest rate, and then slows down from that. On the other hand, the accuracy of the TLC method used did not reach under 0.5 mm liquid distance change, and therefore we could not notice very slow liquid movement to sufficient accuracy. We can conclude, therefore, that at the beginning of the TLC development the water evaporation seems to have a very minimal influence on the eluent rising. During the time the influence was seen to decrease to $0.002 \text{ mm min}^{-1}$, and it is probable that after 40 min development time the evaporation still has only a minor effect on the liquid movement when comparing the influence of wetting force and viscous drag force. Only toward the very end of the experiment can we expect evaporation to be a further equilibrating factor additional to the wetting force-retardation balance.

The balance between the wetting force and the viscous drag determines the rate of progress. As the viscous drag increases in proportion to the length over which the liquid flows within the structure, and decreases to the fourth power of the typical equivalent capillary diameter (Poiseuille effect), there comes a point when the drag equals the wetting force. The Young–Laplace equation (Eq. (1)) [2,7,17,18] describes the wetting force, $\pi r^2 p_c$, of a liquid contacting the walls of a capillary,

$$p_c = \frac{-2\gamma_{lv} \cos \theta_{eq}}{r} \quad (1)$$

where p_c is the Laplace capillary pressure, r the internal capillary radius, γ_{lv} the interfacial tension at the liquid–vapour interface, and θ_{eq} is equilibrium contact angle. During liquid motion, the Young–Laplace pressure drives the liquid against the viscous Poiseuille drag force, given by

$$\frac{dV}{dt} = \frac{\pi r^4}{8\eta l} \Delta P \quad (2)$$

where dV/dt describes the volume flow rate of a liquid of viscosity η through the effective capillary pipe of radius r and length l under the driving pressure difference ΔP .

4.1. Anionic dye–anionic coating

The upper three pictures in Fig. 9 show how water and the anionic dye colorant with water rose through the anionic TLC coating plates during the chromatographic experiment. The gray level becomes darker and darker until, at a certain moment, the liquid has filled the pores of the coating layer that are located within the chosen analyzed area. The turning point in gray value

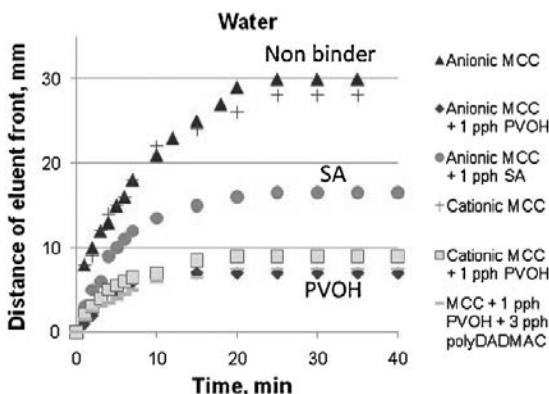


Fig. 8. The distance of eluent (water) front during the time during the chromatographic process.

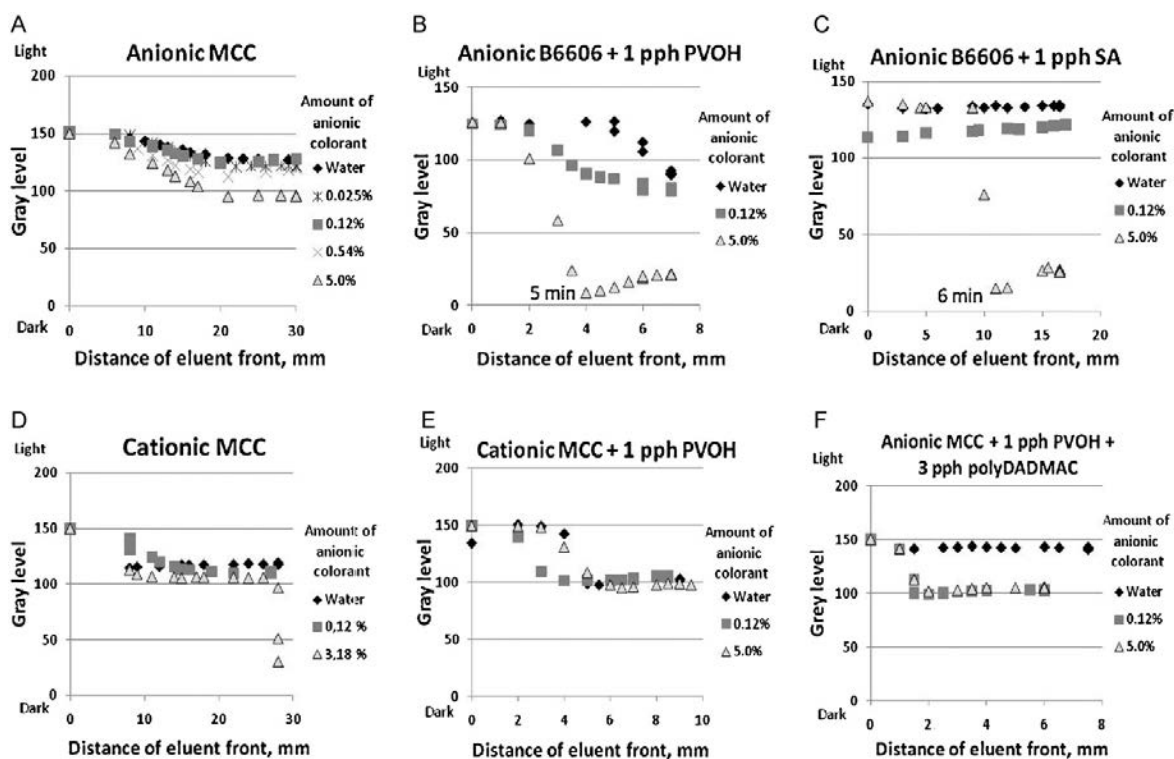


Fig. 9. The gray level values of coatings during the chromatographic sorption process. The content of anionic colorant was adjusted by applying colorant into the water (weight-percent). The measurement of anionic MCC coating had a lower light intensity than the others. A – anionically dispersed MCC, B – anionic MCC with 1 pph PVOH, C – anionic MCC with 1 pph SA latex, D – cationically dispersed MCC, E – cationic MCC with 1 pph PVOH, F – anionic MCC with 1 pph PVOH and 3 pph polyDADMAC.

traversing the analyzed distance takes between 4 min and 6 min with these 100 g m^{-2} coatings. The small size of a water molecule, 0.27–1.00 nm (depending on the amount of molecules in one cluster) [19], enables the capillary flow in the intra-particle pores. The surface of the coating structure first wets and the capillary flow drives the ink vehicle into the small pores. As the amount of ink increases, the permeation flow in larger pores increases so that there are no more air-containing pores which could reflect the light. The size of a colorant molecule is about 1.3 nm (taking account of the length of different bonds in the Cu phthalocyanine colorant molecule and assuming the molecule is planar), which means that the colorant fits well into the 20–70 nm diameter intra-particle pores, provided these pores are accessible. It seems that the col-

orant follows the pigment surfaces and the bridges between the pigment particles almost everywhere.

After the gray value turning points (Fig. 9), where the curves reach the minimum value, the gray level of the plates increases slightly. The anionic dye washes out from the anionic coating layer as the eluent proceeds because there are no chemical groups that can fix the colorant. At high colorant amounts there were more visible changes in gray level values. Real inkjet inks contain about 3–8 wt% of colorant [20], so the use of a 5 wt% solution is within the range of commercial practice. In TLC analysis the amount of liquid is clearly higher than in the real inkjet printing and therefore this washing effect is likely to be less important in practical inkjet ink setting.

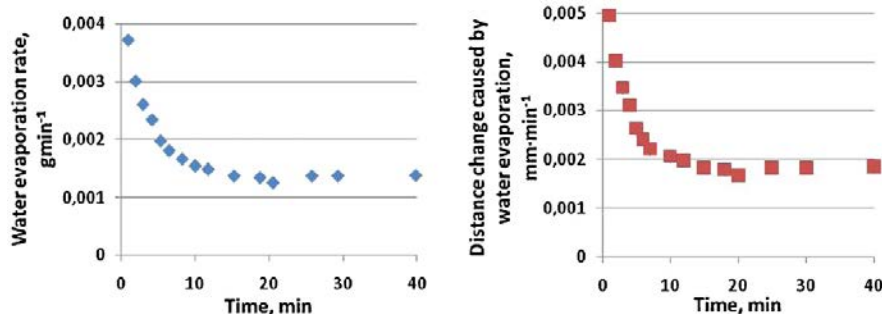


Fig. 10. The evaporation rate of water during the time and from that calculated the effect of water evaporation on the eluent rate through the TLC plate. In the distance evaluation, the coating layer width was 150 mm and thickness $100 \mu\text{m}$ and the porosity of coating layer was taken to be 50%.

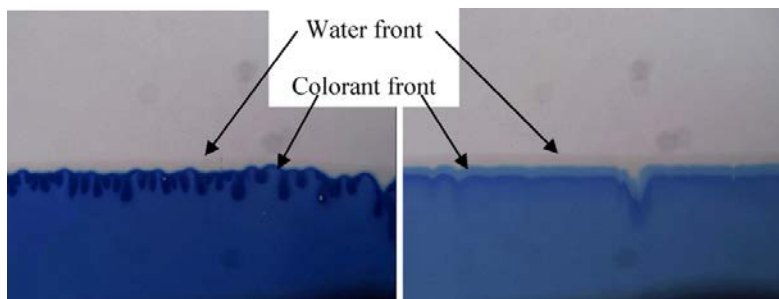


Fig. 11. The water front is seen to be ahead of the colorant front in the anionic coating layers after 4 min: left 5.00 wt% and right 0.54 wt% anionic colorant.

It is also observed that the eluent moves further in the anionic dispersed pigment layer than in 1 pph binder-containing layer. After a distance of 30 mm, there was no further change in the distance travelled in the anionic pigment layer, whereas in the PVOH coating the eluent front stopped after 7 mm, and in the SA coating after 17 mm (Figs. 8 and 9). On the basis alone of the larger pore volume of SA-containing coating, due to structural spacing, we might expect that eluent would rise further than through the non-binder containing coatings. However, the determining factors are a combination of fine pores (driving the capillarity at the wetting front) and the larger pore-throat constructions (defining the minimal flow resistance pathway) in the network structure. Furthermore, the hydrophobicity of latex polymer can act to prevent partially the polar liquid penetration, unlike in the case of hydrophilically dispersed pigment. Furthermore, the PVOH-containing coating had smaller pore diameters than the SA coating, which would promote greater capillary forces acting on the eluent. The smaller pore volume of PVOH coating can have an influence here also, but more likely the hydrophilic interpolymer diffusive nature of PVOH, causing the polymer to swell, closes the nano-size pores so that eluent cannot rise through further through the structure.

The 1 pph binder addition slightly decreases the porosity and the average pore diameter of PVOH coating (Figs. 4 and 5). On the other hand, PVOH is a hydrophilic binder, and the swelling of PVOH (absorption by such a binder film is shown to be 30.2% [21]) changes the accessible amount/size/volume of small pores during the water absorption process [21]. A rough estimation of swelling effects indicates that the uniform layer of 1 pph PVOH (density 1.26 g cm^{-3}) produces a 0.17 nm thick binder layer on the surface of the pigment ($46.2 \text{ m}^2 \text{ g}^{-1}$ specific surface area) and the swelling increases the thickness to 0.26 nm. Thus, PVOH can decrease and even block the nano-size pores of coating layer, and so reduce the capillary driving force, although this will be replaced by the diffusion potential as water diffuses between the polymer chains.

However, the results of mercury porosimetry indicate that the SA containing coating had a little higher porosity and larger pores than the pigment structure without binder. The higher pore volume would suggest that SA coating could transport liquid further than the lower pore volume structure. The SA latex swells only a few percent under the influence of water [21]. Thus, the capillary flow controls the water imbibitions in SA containing coatings. The difference between the dispersed pigment coating and the SA latex containing coating is suggested to be caused by the difference in the hydrophilic nature. The SA latex has hydrophobic nature, which means that the contact angle of polar liquid increases and thus the capillary pressure of pores decreases. The hydrophobicity is mediated probably by the surfactant and/or carboxylation used to stabilize the latex, whereas the dispersing agent in the case of the pigment has produced a hydrophilic structure [22]. Altogether, the equilibrium point, at which the capillary and permeability forces

balance, comes much sooner with binder containing coatings, both due to physical connectivity and due to surface chemistry effects, and these are reflected in the distance the liquid front finally travels.

Fig. 11 shows that, in the case of an anionic coating, the water molecules form a wetting front and the anionic colorant front follows behind it. If the speed of eluent in the plate is taken into account, we see that the wetting front is from 30 s to a few minutes ahead of the ink colorant front, depending on the coating layer pore structure and interaction with binder. In the case of coated paper, we assumed that the liquid is moving in the z-direction of the coating structure in a quite similar way as in the TLC coating layers studied, i.e. the ink is moving with constant speed in the coating layer, the thickness of the coating layer is between 10 and $20 \mu\text{m}$, and the absorption time of the layer is about 300 ms (as measured by DIGAT) [21]. This would mean that the wetting front is somewhere between $\sim 0.1 \mu\text{m}$ and $\sim 10 \mu\text{m}$ ahead of the colour front, depending on coating thickness.

Fig. 11 shows also that the colorant concentration is increased at the colorant front. The mechanism is, therefore, assumed to be one of anionic repulsion from the finest pores, allowing the water to imbibe into these pores, but not the dye. This also explains why the water fastness of anionic coatings for anionic dyes is so poor [23], because the dye cannot be protected from the external water flow as it is concentrated in the inter-particle voids that constitute the permeable pathway during washing. The anionic dye cannot adsorb onto the anionic surface because of charge repulsion.

4.2. Anionic dye–cationic coating

In the cationic coating layer, the anionic dye becomes fixed to the cationic surface, being drawn by the electrostatic interactions (ionic concentration and Coulombic force). This results in a concentration of dye right at the start position in the TLC experiment, and this observation agrees with many other equivalent results, such as those in [12,20,23–26]. The gray level decreases in Fig. 9 from 150 to 100, because the detected area fills with water. When the surface, available for colorant adsorption, is saturated, the colorant migrates further with the eluent liquid (Fig. 7). This could also be noticed in Fig. 9, where the gray value results dropped from the 100 gray level to the level of 30 with the highest colorant amount in the cationic MCC coating. The gray values of cationic MCC decreases in the distance of 28 mm because the anionic colorant started to rise to the detection area.

5. Conclusions

The results show that even a surprisingly small amount of binder affects the liquid transfer along the MCC pigment coating layers. The capillary flow drives the liquid into the coating structure. On

the other hand, the polar liquid (water) diffuses into hydrophilic binder polymers and acts as a swelling agent, causing closure of some pores and a reduction generally of pore diameters. This acts on the short timescale liquid absorption, due to the short nano distances involved in the finest pores despite being a diffusion process, but reduces the available volume. The balance between the wetting force and the viscous drag determines the rate of progress. The permeation flow is the main resistance determining factor to the capillary and diffusion controlled driving force in the continuing liquid mass transfer.

The results of SA latex containing coatings show that the hydrophobic nature of latex prevents the diffusion of the polar liquid into the structure of the binder layer matrix, but wetting still occurs probably related to the surfactant and/or carboxylation used to stabilize the latex. Also, the SA latex coating carries water further along a TLC plate than in the PVOH containing. The slightly larger pores of the SA containing coating structure allow for quicker liquid penetration, rather than the smaller pores and reduced connectivity of the PVOH containing coatings.

References

- [1] J. Kettle, T. Lamminmäki, P. Gane, A review of modified surfaces for high speed inkjet coating, *Surface and Coating Technology* 204 (12) (2010) 2103–2109.
- [2] L. Agbezuge, Drying of ink jet images on plain papers – falling rate period, in: IS&T's NIP7: International Conference on Digital Printing Technologies, Portland, USA, 1991, pp. 173–184.
- [3] M. von Bahr, F. Tiberg, B. Zhmud, Oscillations of sessile drops of surfactant solutions on solid substrates with differing hydrophobicity, *Langmuir* 19 (24) (2003) 10109–10115.
- [4] F. Girard, P. Attané, V. Morin, A new analytical model for impact and spreading of one drop: application to inkjet printing, *Tappi Journal* 5 (12) (2006) 24–32.
- [5] C.J. Ridgway, P.A.C. Gane, Controlling the absorption dynamic of water-based ink into porous pigmented coating structures to enhance print performance, *Nordic Pulp and Paper Research Journal* 17 (2) (2002) 119–129.
- [6] M. von Bahr, J. Kizling, B. Zhmud, F. Tiberg, Spreading and penetration of aqueous solutions and water-borne inks in contact with paper and model substrates, in: *Advances in Printing Science and Technology – Advances in Paper and Board Performance*, 27th Research Conference of the International Association of the Research Institutes for the Printing, Information and Communication Industries, Graz, Austria, September 10–13, 2000, pp. 88–102.
- [7] G. Desie, G. Deroover, F. De Voeght, A. Soucemarianadin, Printing of dye and pigment-based aqueous inks onto porous substrates, *Journal of Imaging Science and Technology* 48 (5) (2004) 389–397.
- [8] M. von Bahr, F. Tiberg, B. Zhmud, Spreading dynamics of surfactant solutions, *Langmuir* 15 (15) (1999) 7069–7075.
- [9] K.L. Yip, A.R. Lubinsky, D.R. Perchak, K.C. Ng, Measurement and modelling of drop absorption time for various ink-receiver systems, *Journal of Imaging Science and Technology* 47 (5) (2003) 388–393.
- [10] T.T. Lamminmäki, J.P. Kettle, P.J.T. Puukko, C.J. Ridgway, P.A.C. Gane, The role of ink component diffusion during absorption into inkjet coatings, in: *11th Advanced Coating Fundamentals Symposium*, Munich, Germany, October 11–13, 2010, pp. 195–214.
- [11] C.J. Ridgway, P.A.C. Gane, The impact of pore network structure on the absorption of pigmented inkjet inks, in: *Tappi Coating Conference*, Toronto, Ontario, Canada, Session 6, April 17–20, 2005, 15 pp.
- [12] D.W. Donigian, P.C. Wernett, M.G. McFadden, J.J. McKay, Ink jet dye fixation and coating pigments, in: *TAPPI Coating Conference 1998*, New Orleans, USA, Tappi Press, Atlanta, USA, May 4–6, 1998, pp. 393–412.
- [13] D.W. Donigian, P.C. Wernett, M.G. McFadden, J.J. McKay, Ink-jet dye fixation and coating pigments, *Tappi Journal* 82 (8) (1999) 175–182.
- [14] D. Glittenberg, A. Voigt, D. Donigian, Novel pigment–starch combination for the online and offline coating of high-quality inkjet papers, *Paper Technology* 44 (7) (2003) 36–42.
- [15] P.A. Gane, J.P. Kettle, G.P. Matthews, C.J. Ridgway, Void space structure of compressible polymer spheres and consolidated calcium carbonate paper-coating formulations, *Industrial and Engineering Chemistry Research* 35 (5) (1996) 1753–1764.
- [16] P.A.C. Gane, M. Salo, J.P. Kettle, C.J. Ridgway, Comparison of Young–Laplace pore size and microscopic void area distributions in topologically similar structures: a new method for characterising connectivity in pigmented coatings, *Journal of Materials Science* 44 (2) (2009) 422–432, doi:10.1007/s10853-008-3134-8.
- [17] J. Schoelkopf, C.J. Ridgway, P.A.C. Gane, G.P. Matthews, D.C. Spielmann, Measurement and network modeling of liquid permeation into compacted mineral blocks, *Journal of Colloid and Interface Science* 227 (1) (2000) 119–131.
- [18] C.J. Ridgway, P.A.C. Gane, J. Schoelkopf, Effect of capillary element aspect ratio on the dynamic imbibition within porous networks, *Journal of Colloid and Interface Science* 252 (2002) 373–382.
- [19] D. Topgaard, O. Söderman, Diffusion of water absorbed in cellulose fibers studied with H-NMR, *Langmuir* 17 (9) (2001) 2694–2702.
- [20] S. Pond, *Inkjet Technology and Product Development Strategies*, USA, 2000, 406 pp.
- [21] T. Lamminmäki, J. Kettle, P. Puukko, P.A.C. Gane, C. Ridgway, Inkjet print quality: the role of polyvinyl alcohol upon structural formation of CaCO₃ coatings, in: *International Paper and Coating Chemistry Symposium*, Hamilton, Canada, June 10–12, 2009, 13 pp.
- [22] P.A.C. Gane, C.J. Ridgway, Moisture pickup in calcium carbonate coating structures: role of surface and pore structure geometry, in: *TAPPI 10th Advanced Coating Fundamentals Symposium*, Montreal, Canada, Tappi Press, Atlanta, USA, June 10–13, 2008, 24 pp.
- [23] K. Vikman, T. Vuorinen, Water fastness of ink jet prints on modified conventional coatings, *Journal of Imaging Science and Technology* 48 (2) (2004) 138–147.
- [24] A. Lavery, J. Provost, Color-media interactions in ink jet printing, in: IS&T's NIP13: International Conference on Digital Printing Technologies, Seattle, Washington, USA, November 2–7, 1997, pp. 437–442.
- [25] K. Vikman, T. Vuorinen, Light fastness of ink jet prints on modified conventional coatings, *Nordic Pulp and Paper Research Journal* 19 (4) (2004) 481–488.
- [26] T. Kallio, J. Kekkonen, P. Stenius, Acid/base properties and adsorption of an Azo dye on coating pigments, *Journal of Dispersion Science and Technology* 27 (September) (2006) 825–834.